金星熱圏GCM(Hoshino et al., 2012, 2013)の確認と活用

Hiroki Karyu[a], Takeshi Kuroda[a], Hideo Sagawa[b], Hitoshi Fujiwara[c], Masahiro Takagi[b], Yasumasa Kasaba[a]

[a] Tohoku University, [b] Kyoto Sangyo University, [c] Seikei University

Outline

- ❑ Upper atmospheric dynamics of Venus
- ❑ Hoshino et al. (2012)
- ❑ Hoshino et al. (2013)
- ❑ Test runs and applications

Upper atmospheric dynamics of Venus

Overview

❑ Different dynamical regimes

1. Retrograde superrotationg zonal wind (RSZ wind)
2. Subsolar-to-antisolar wind (SS-AS wind)

➢ ~ 70 km → RSZ wind

➢ 70 ~ 120 km → transition region

➢ 120 km ~ SS-AS circulation

Transition region shows large variability

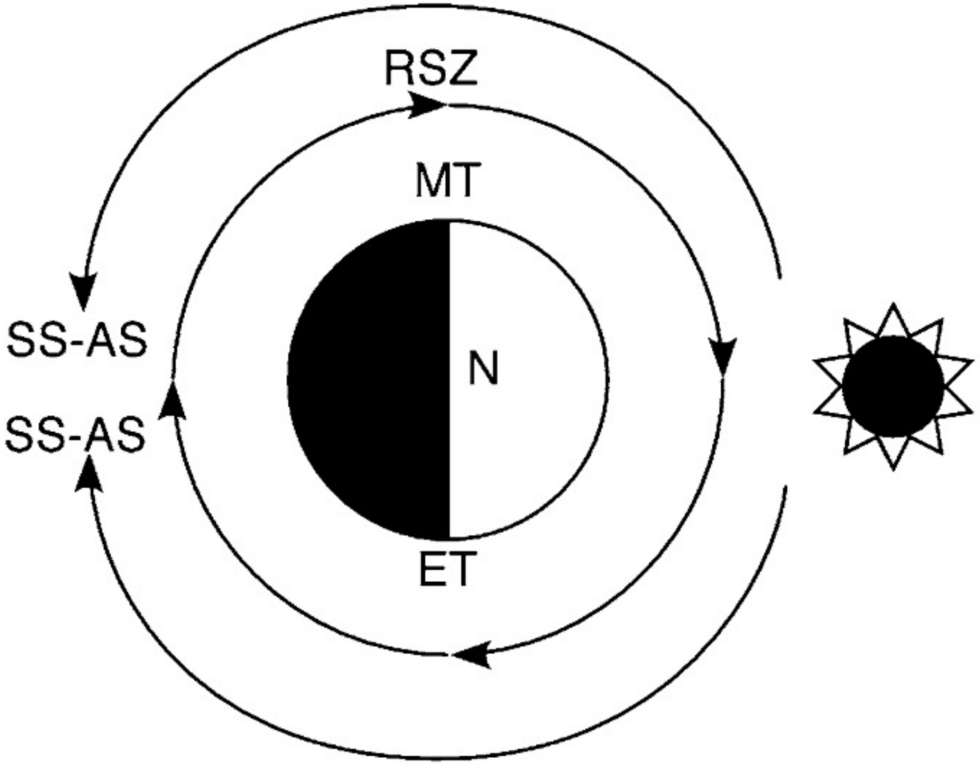

Brecht et al., 2011

Observational studies : Nightglow

O2 Center : antisolar point NO

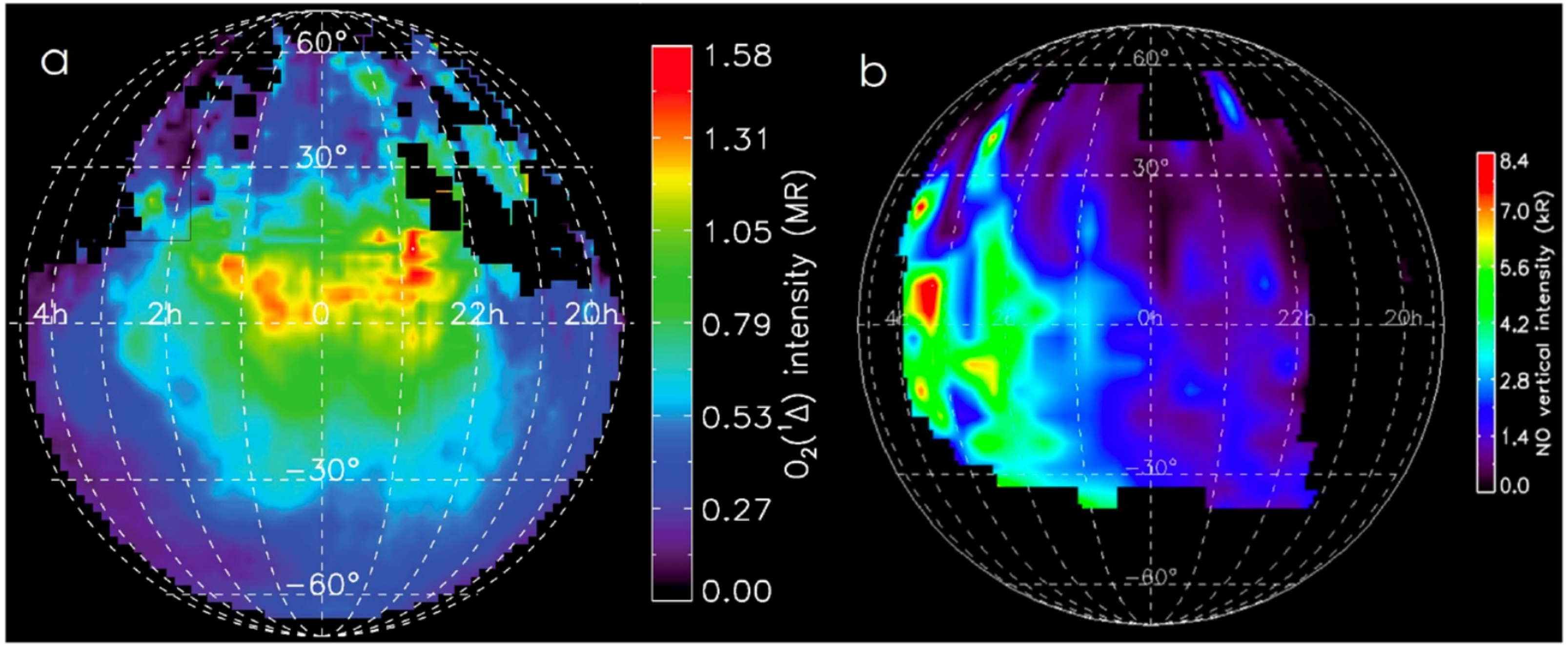

Maps of the statistical distribution of the O_2 and NO night glow [Soret et al., 2012, Stiepen et al., 2013]

O_2 peak : 99 km
NO peak : 115 km

→ different global circulation pattern

99 km : Stable
115 km : Zonal wind

Patchy structure indicates high variability of O_2 and NO night glow intensity peak
→ variation in the background wind?

Observational studies : Wave activity

- ❑ Periodic variations of oxygen EUV dayglow in the thermosphere [Masunaga et al., 2015]

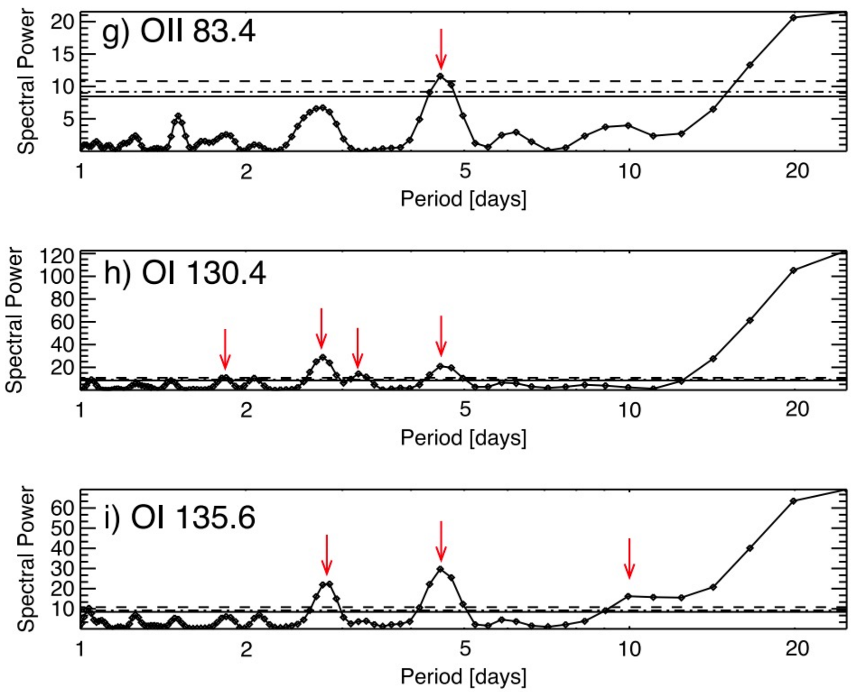

- 1.8, 2.8, 3.1, 4.5, and 9.9 day period

- ❑ Density oscillation in the nightside of the thermosphere [Forbes and Konopliv, 2007]

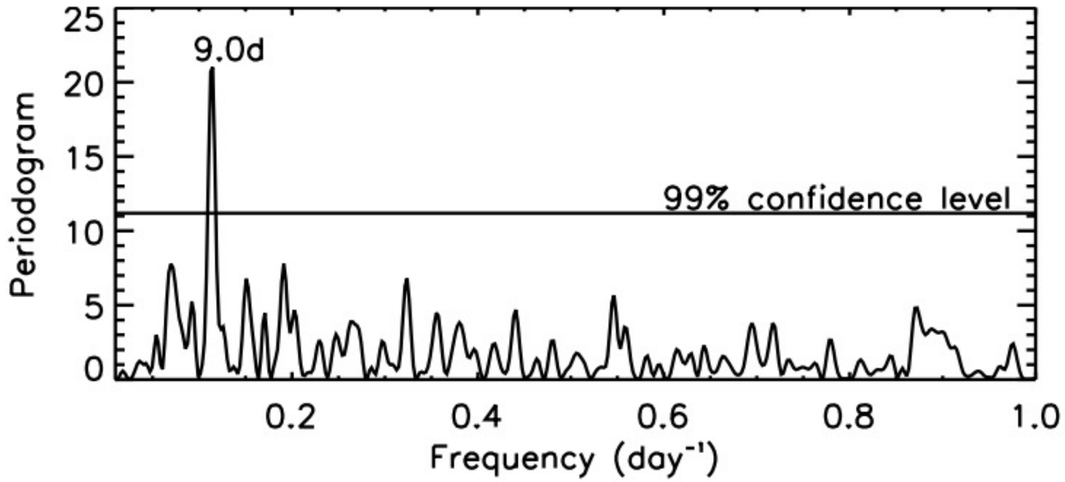

- 9 day period

Density oscillation of by planetary-scale waves and/or gravity waves propagating from the middle atmosphere?

Summary of wind measurements

Species/Emissions/Temperatures	Altitude (km)	SS-AS Winds (m/sec)	RSZ Winds (m/sec)
Visible Spectroscopy (Solar Radiation)[a]	$\sim$70		83 $\pm$ 27
Temperatures (IR and Occultation)[b]	70–90		Variable (weak)
CO mm, CO distribution[c]	$\sim$80–100	Present	Variable
CO mm, winds[d]	$\sim$90–105	$\leq$40–322 $\pm$ 25	35–147 $\pm$ 3 (variable)
10-micron, CO_2 heterodyne[e]	109 $\pm$ 10	$\leq$35–129 $\pm$ 1	3 $\pm$ 7–40 $\pm$ 3 (weak)
O_2 IR (1.27 microns)[f]	90–110		Variable ($\sim$10–50)
O_2 Visible (400–800 nm)[g]	100–130		Weak ($\leq$30)
CO 4.7-micron, winds[h]	125–145	Sum = 200 $\pm$ 50	
NO nightglow (UV)[i]	115–150	$\sim$200	40–60
O dayglow (130 nm)[j]	130–250		Eddy diffusion constraint
Temperatures (night)[k]	Above 150	$\sim$200	$\sim$50–100
H dayglow (121.6 nm)[l]	Above 150		$\sim$45–90
H and He densities[m]	Above 150		$\sim$45–90

~70 km : RSZ

70 ~ 120 km : Variable

120 ~ : SS-AS (& RSZ)

Schubert et al., 2007

Outstanding problems

- ❑ Wind variations between 90 and 130 km regions

- ❑ Variable structures of NO and O_2 nightglow emissions
  → Non-steady transport of these species?
  → Influence of gravity waves?

- ❑ The role of wave activity

Hoshino et al. (2012) → Rossby wave, Kelvin wave, Thermal tides
Hoshino et al. (2013) → Gravity wave

Hoshino et al. (2012)

Model description

❑ Basic settings

- 5° in longitude x 10° in latitude,
- 38 vertical layers (80~180 km)
- Chemical reactions (CO, CO_2, O, O_2)

Chemical reactions

Reaction	Reaction coefficient	Reference
$CO_2 + h\nu \rightarrow CO + O$	J	
$O + O + CO_2 \rightarrow O_2 + CO_2$	$k_{11} = 5.2 \times 10^{-47} exp(900/T)\ m^6\ s^{-1}$	Hampson (1980)
$CO + O + CO_2 \rightarrow CO_2 + CO_2$	$k_{12} = 6.2 \times 10^{-48}\ m^6\ s^{-1}$	Slanger et al. (1972)

- 1-D nightglow model

→ calculated with 3-D composition distribution obtained by the GCM

→ comparison with previous observations

Recombination of atomic oxygen

\+

$$ClO + O \rightarrow O_2^* + Cl \quad (26)$$
$$HO_2 + O \rightarrow O_2^* + OH \quad (27)$$
$$ClO_2 + Cl \rightarrow O_2^* + Cl_2. \quad (28)$$

Model description : Basic equations

- Momentum equations

$$\frac{\partial u}{\partial t} = -\mathbf{v}\cdot\nabla u + \left(2\Omega + \frac{u}{r\cos\theta}\right)v\sin\theta - \frac{1}{r\cos\theta}\frac{\partial\Phi}{\partial\phi} + g\frac{\partial}{\partial p}\left(\mu\frac{p}{H}\frac{\partial u}{\partial p}\right) - \lambda_{RF}u, \tag{2}$$

$$\frac{\partial v}{\partial t} = -\mathbf{v}\cdot\nabla v - \left(2\Omega + \frac{u}{r\cos\theta}\right)u\sin\theta - \frac{1}{r}\frac{\partial\Phi}{\partial\theta} + g\frac{\partial}{\partial p}\left(\mu\frac{p}{H}\frac{\partial v}{\partial p}\right) - \lambda_{RF}v, \tag{3}$$

μ : Viscous coefficient
λ_{RF} : Rayleigh friction coefficient

- Continuity equation

$$\frac{\partial\omega}{\partial p} = -\frac{1}{r\cos\theta}\frac{\partial(v\cos\theta)}{\partial\theta} - \frac{1}{r\cos\theta}\frac{\partial u}{\partial\phi}, \tag{9}$$

- Eddy viscosity

$$\mu_e = \rho K \tag{4}$$

$$K = \begin{cases} K_0\left(\frac{p}{p_{turbo}}\right)^{-0.5} & (p \geqslant p_{turbo}) \\ K_0 & (p < p_{turbo}) \end{cases}, \tag{5}$$

- Molecular viscosity

$$\mu_m = \sum_{i=1}^{3}\frac{\mu_i}{\left(\frac{1}{N_i}\right)\sum_{j=1}^{3}N_j\phi_{ij}}, \tag{6}$$

$$\phi_{ij} = \frac{\left\{1 + \left(\frac{\mu_i}{\mu_j}\right)^{1/2}\left(\frac{M_j}{M_i}\right)^{1/4}\right\}^2}{2\sqrt{2}\left(1 + \frac{M_i}{M_j}\right)^{1/2}}, \tag{7}$$

- Rayleigh friction

$$\lambda_{RF} = \begin{cases} \lambda_0\frac{2}{1+(p/p_{turbo})^{0.5}} & (p \geqslant p_{turbo}) \\ \lambda_0 & (p < p_{turbo}) \end{cases}, \tag{8}$$

Model description : Energy conservation

- Energy conservation

$$\frac{\partial \epsilon}{\partial t} = \underbrace{-\mathbf{v}\cdot\nabla(\epsilon+gz)}_{1} + \underbrace{g\frac{\partial}{\partial p}\left(K_m \frac{p}{H}\frac{\partial T}{\partial p}\right) + g\frac{\partial}{\partial p}\left\{K_T\left(\frac{p}{H}\frac{\partial T}{\partial p} - \frac{g}{C_p}\right)\right\}}_{2} + \underbrace{\left(\frac{K_m+K_T}{\rho}\right)\left(\frac{1}{r^2 cos^2\theta}\frac{\partial^2 T}{\partial \phi^2} + \frac{1}{r^2}\frac{\partial^2 T}{\partial \theta^2} - \frac{tan\theta}{r^2}\frac{\partial T}{\partial \theta}\right)}_{3} + \underbrace{ug\frac{\partial}{\partial p}\left(\mu\frac{p}{H}\frac{\partial u}{\partial p}\right) + vg\frac{\partial}{\partial p}\left(\mu\frac{p}{H}\frac{\partial v}{\partial p}\right)}_{4} + \underbrace{Q_{EUV} + Q_{NIR} + Q_{15\mu m}}_{5}, \quad (11)$$

1. Advectionvertical molecular heat conduction
2. Vertical molecular heat conduction and eddy heat transport
3. Horizontal molecular heat conduction and eddy heat transport
4. Work done by viscous force
5. Solar EUV heating, solar NIR heating, and CO_2 15 μm radiative cooling

Molecular heat conduction coefficient

$$K_m = \sum_{i=1}^{3} \frac{K_i}{\left(\frac{1}{N_i}\right)\sum_{j=1}^{3} N_j \phi_{ij}}, \quad (12)$$

Model description : Boundary conditions

❑ Lower boundary

- Fixed temperature and 0 wind velocity
- [Case 1] Uniform geopotential height
- [Case 2] Geopotential height fluctuation
  → Wave effects
  Similar manner to Bougher et al. (1993)

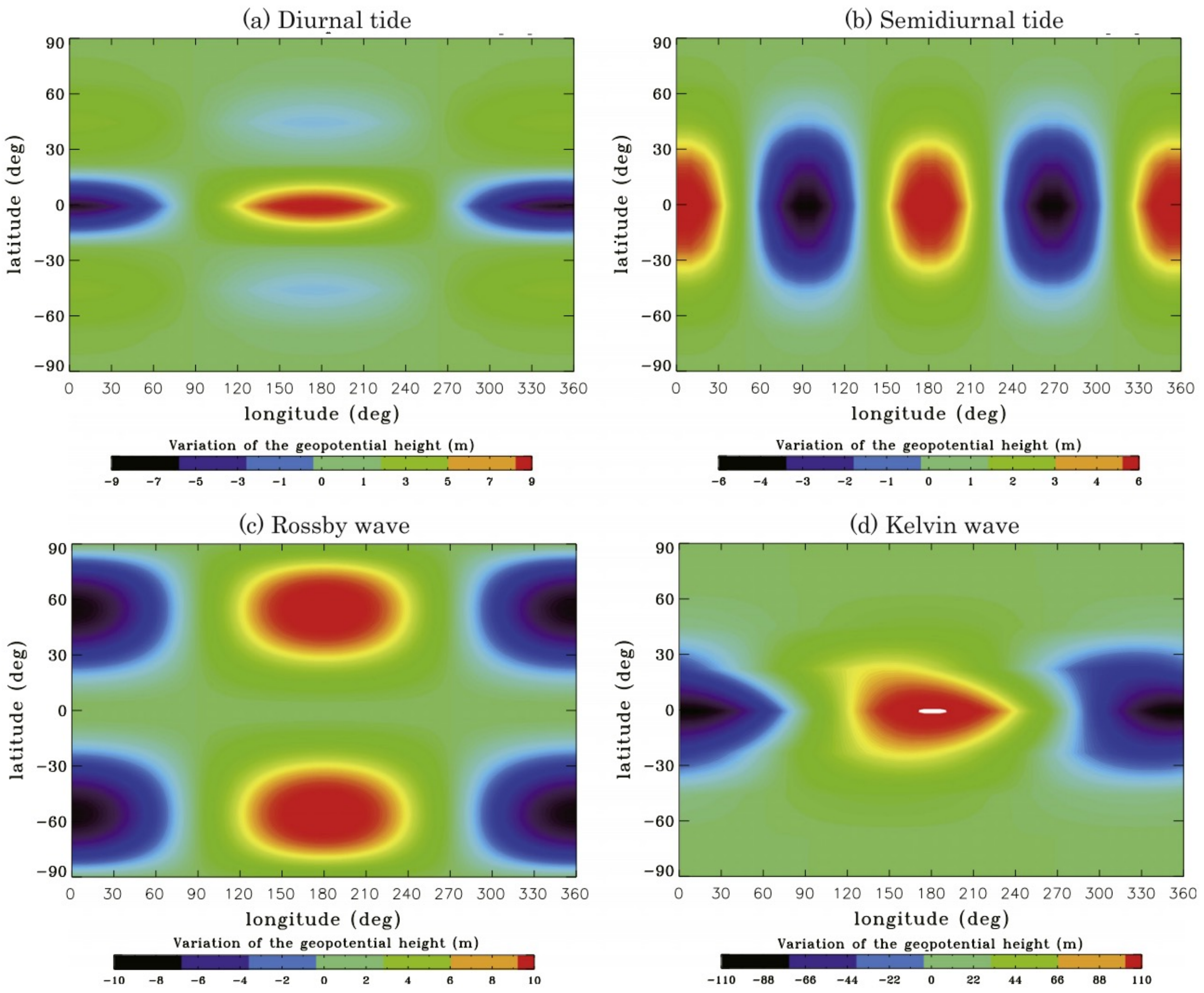

❑ Upper boundary

- No temperature and horizontal wind gradient

Results

Zonal wind [m/s]

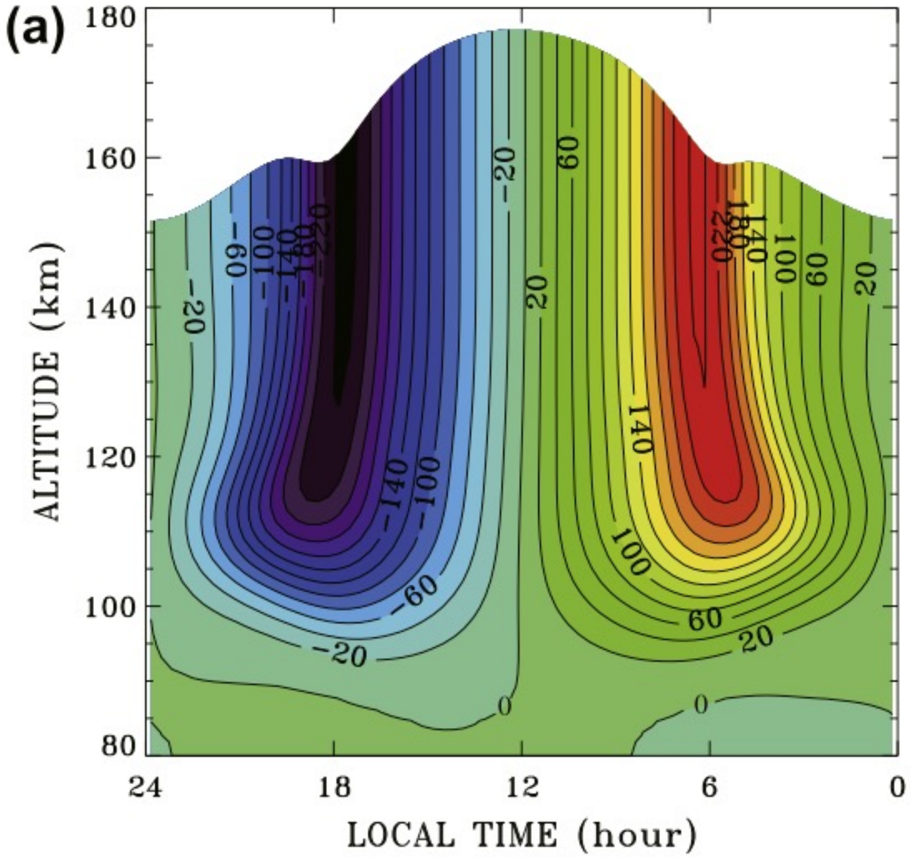

Temperature [K]

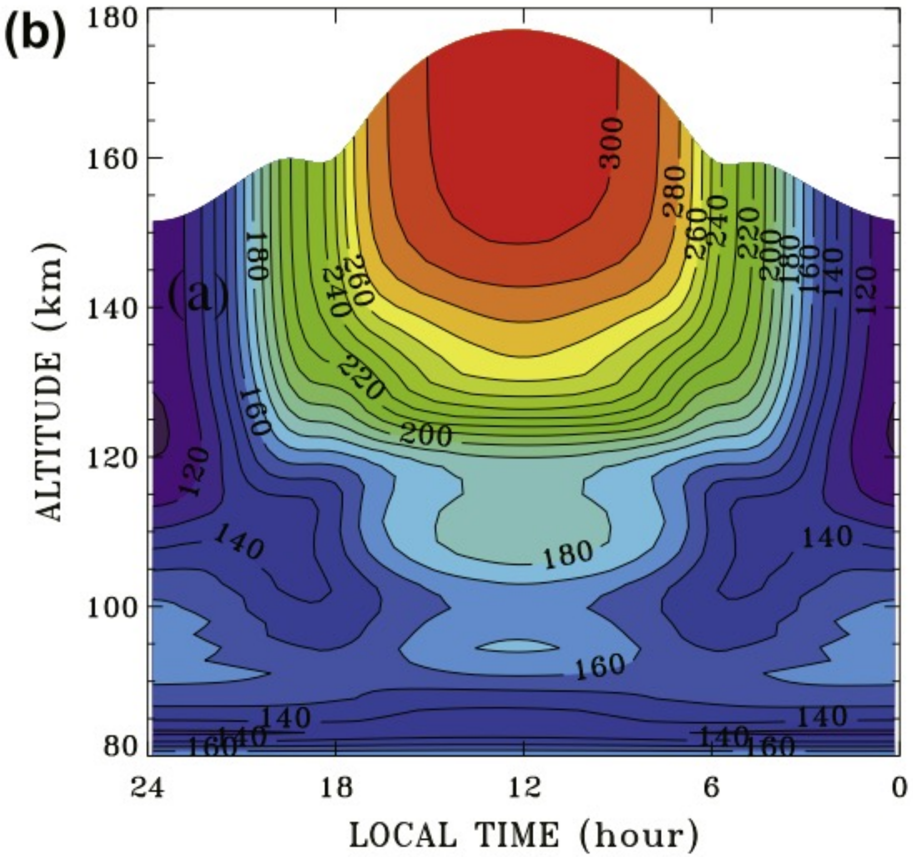

- SS-AS circulation driven by day-night temperature difference due to EUV heating(100 km ~)
- Return flow below 90 km

Effects of atmospheric waves

- Zonal wind average on the cordinates moving with the wave source

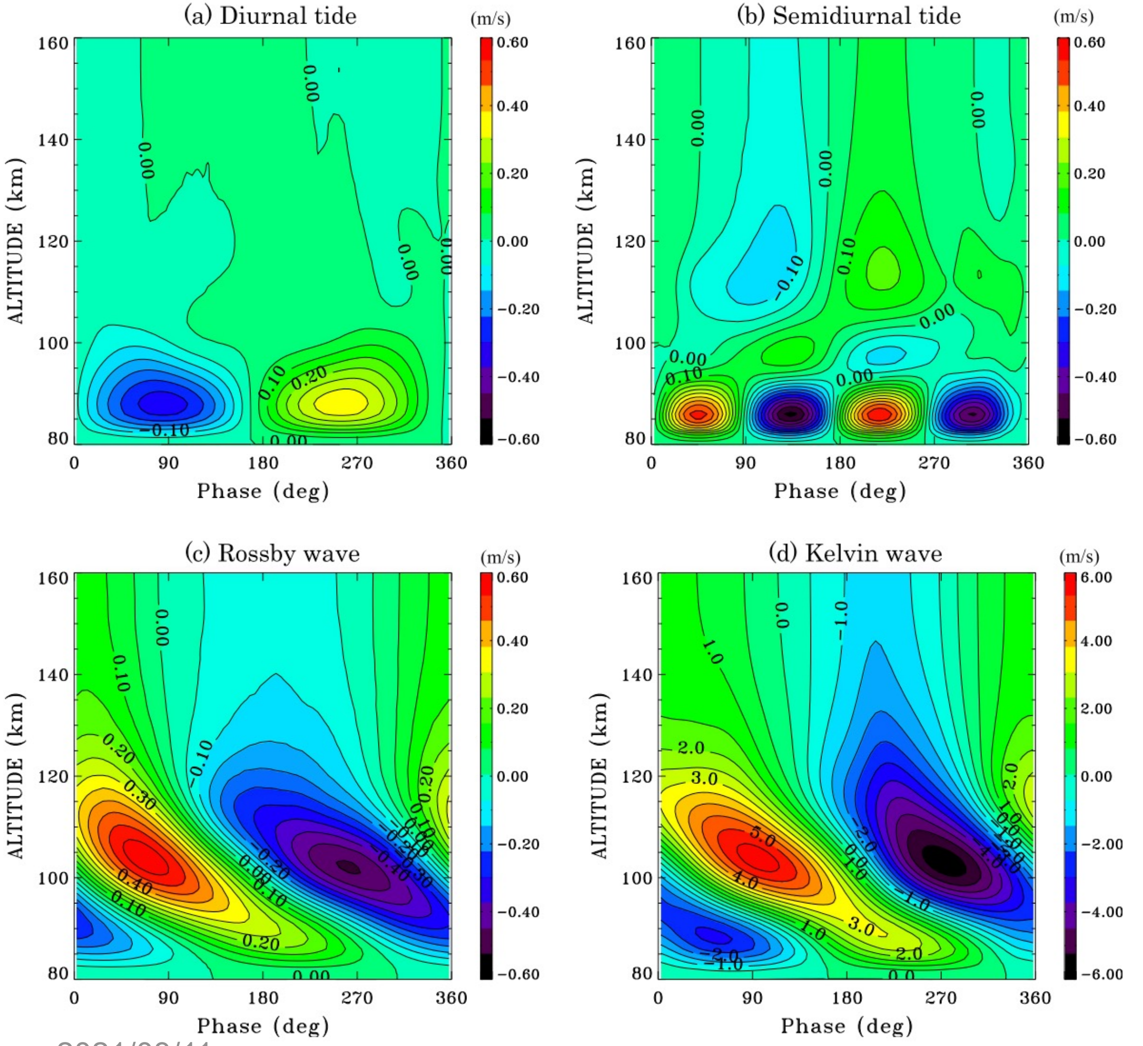

Wave	Vertical wavelength (km)	Period (days)	T_{max} (K)	u_{max} (m/s)
Diurnal tide	Standing wave	117	0.3 (at 85 km)	0.4 (at 87 km)
Semi-diurnal tide	Standing wave	117	1.0 (at 85 km)	0.6 (at 85 km)
Rossby wave	49	5	0.4 (at 95 km)	0.6 (at 105 km)
Kelvin wave	46	4	2.5 (at 95 km)	6.0 (at 105 km)

- Thermal tides do not propagate vertically
- Rossby wave propagates vertically but has small amplitude
- Kelvin wave propagates vertically and has large amplitudes
  (sometimes larger than 10 m/s)

Nightglow distribution

❑ Averaged horizontal distribution of nightglow intensity

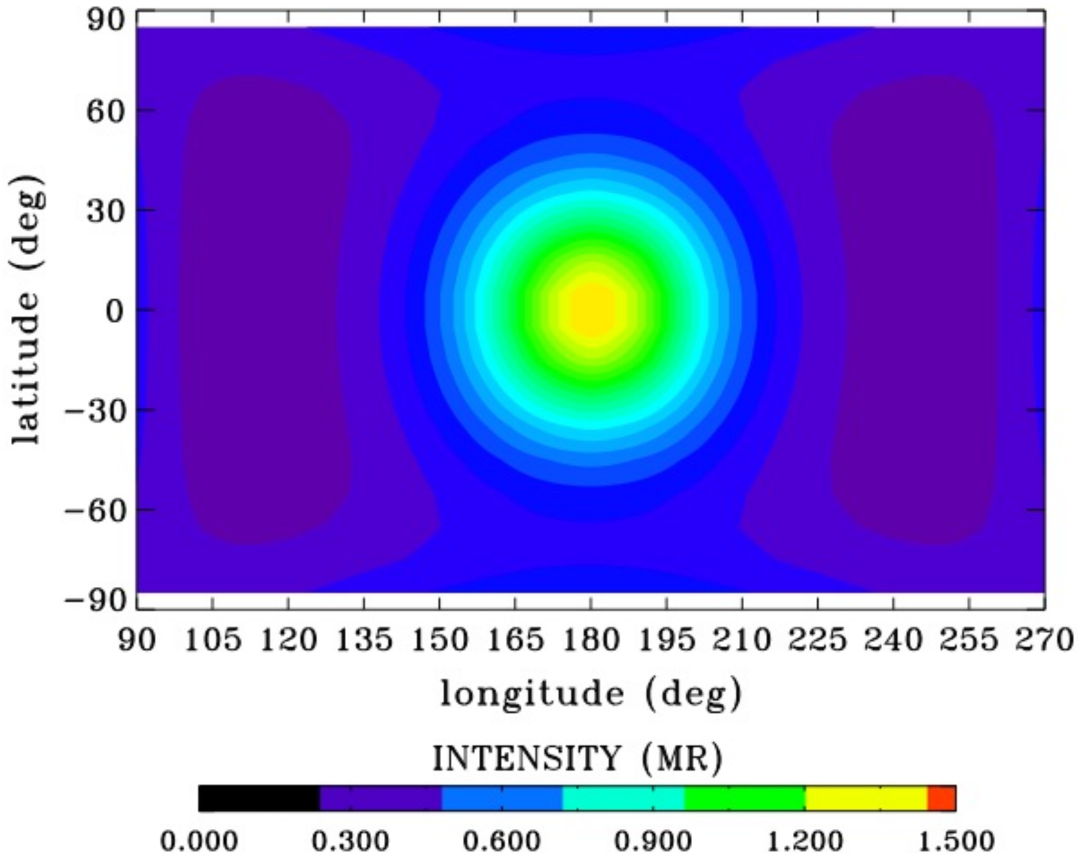

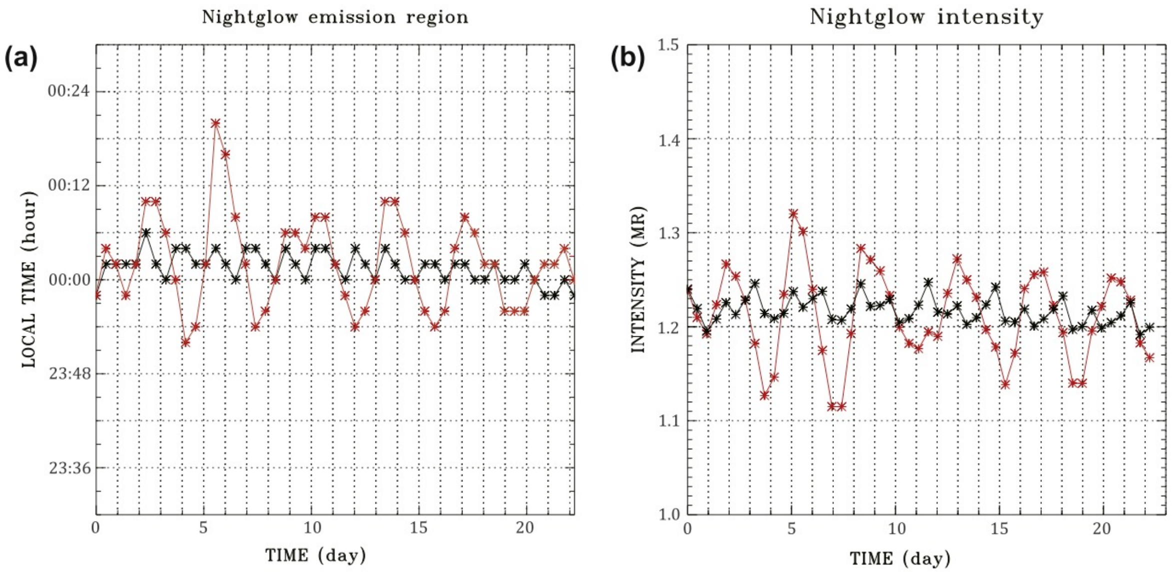

** : without waves, ** : with waves

- Approximately 4 day period fluctuation
→ Period of Kelvin waves

- Observed muximum intensity of 1.2 MR (Piccioni et al., 2009) is consistent with observation

Kelvin wave would be the most plausible cause for temporal variation in the nightglow intensity and distribution

Hoshino et al. (2013)

Model description

- Same basic equations as Hoshino et al. (2012)

- Gravity wave parameterization
  - MK scheme [Medvedev and Klaassen, 2000]

  Momentum deposition by gravity wave with wave number m

$$a_m = -\frac{\beta_m k_h S_m}{m},$$

Convective dumping rate
$\rightarrow$ maximum when $c = \overline{u}$

Horizontal wave nuber

Power-spectral density

Total momentum deposition

$$A = \int_0^\infty a_m \mathrm{d}m.$$

- Lower boundary condition

  1) Fixed zonal wind speed [0 and 40 m/s] (superrotation is considered)
  $\rightarrow$ Center of the gravity wave phase velocity

  2) Power spectrum of gravity waves (vertical wave number)

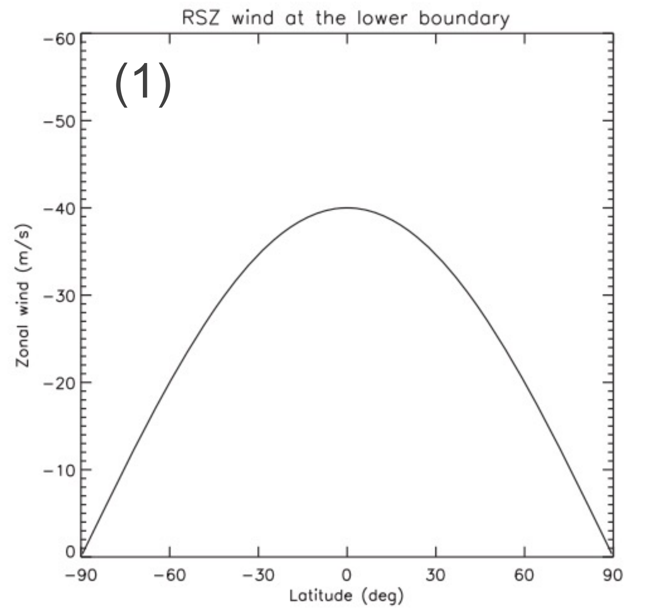

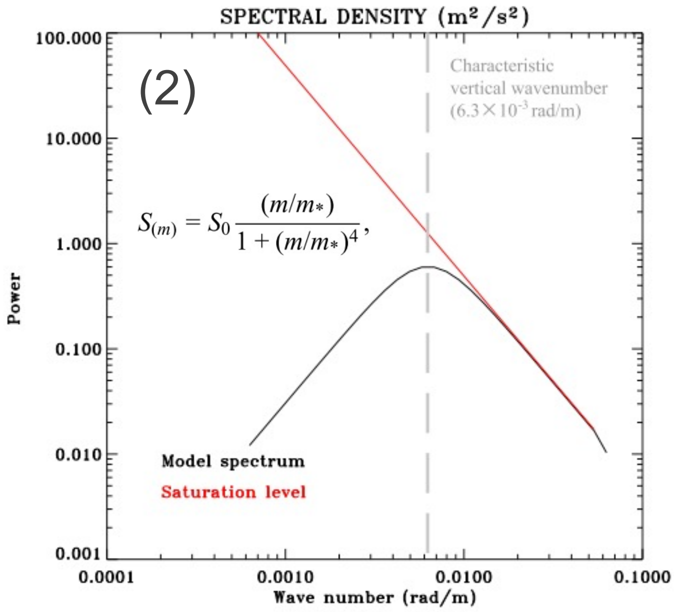

Results : Wind distribution

- ❑ Lower boundary 0 m/s

EQ

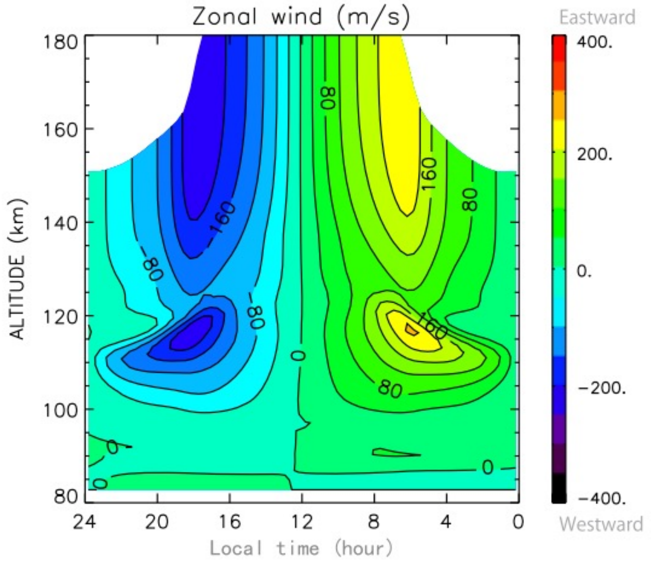

- Symmetric structure with maximum velocity around 240 m/s

- Strong deceleration around 125 km
→ wave drag becomes stronger above 125 km

- ❑ Lower boundary 40 m/s

EQ

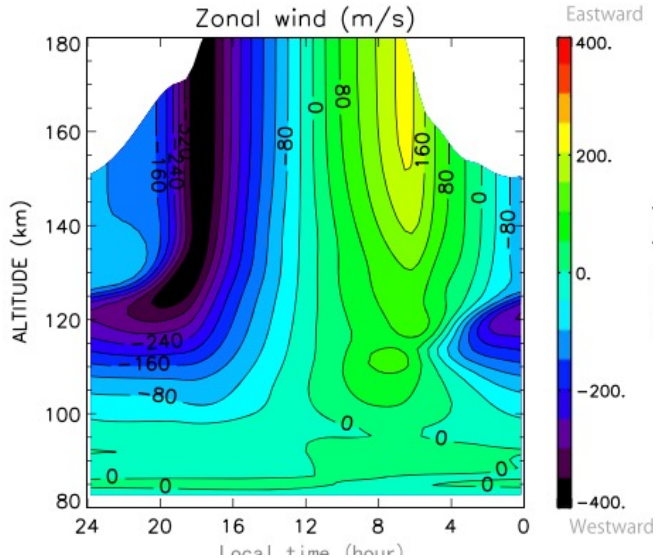

Zonal mean

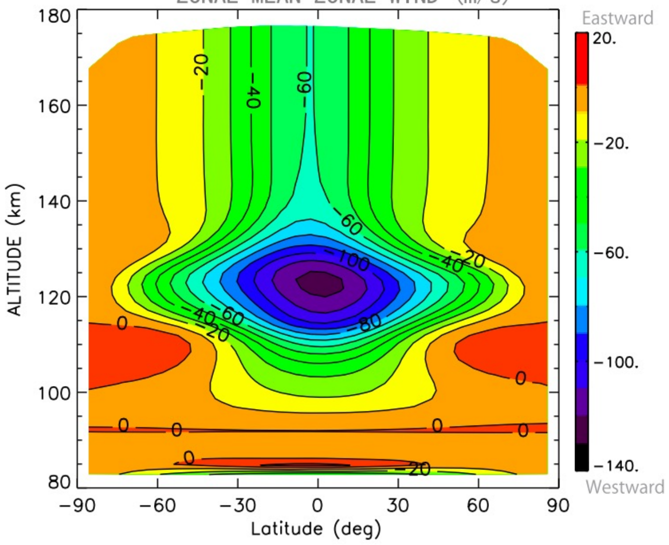

- Complex structure
→ superposition of RSZ and SS-AS wind

- RSZ wind driven by momentum deposition of gravity wave
→ gravity waves with fast phase velocity can reach high altitudes

Results : Nightglow distribution

- Lower boundary 0 m/s

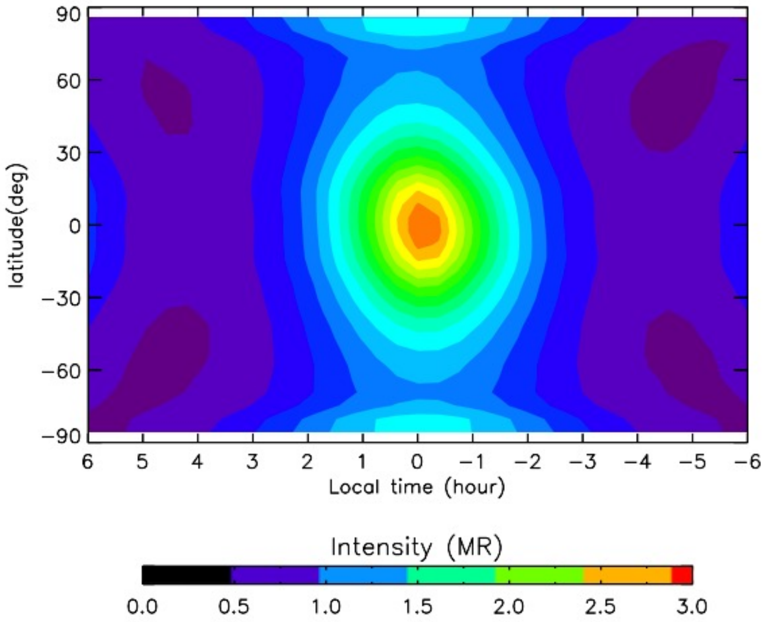

- Comparison with Hoshino et al. (2012)

RMS : $\sigma = \left(\sum_{i}^{M} < u_i^2 > \right)^{1/2}$,

Kelvin wave : 3 m/s
Gravity wave : 8 m/s

Gravity wave would cause stronger temporal variation of the O_2 nightglow

- Lower boundary 40 m/s

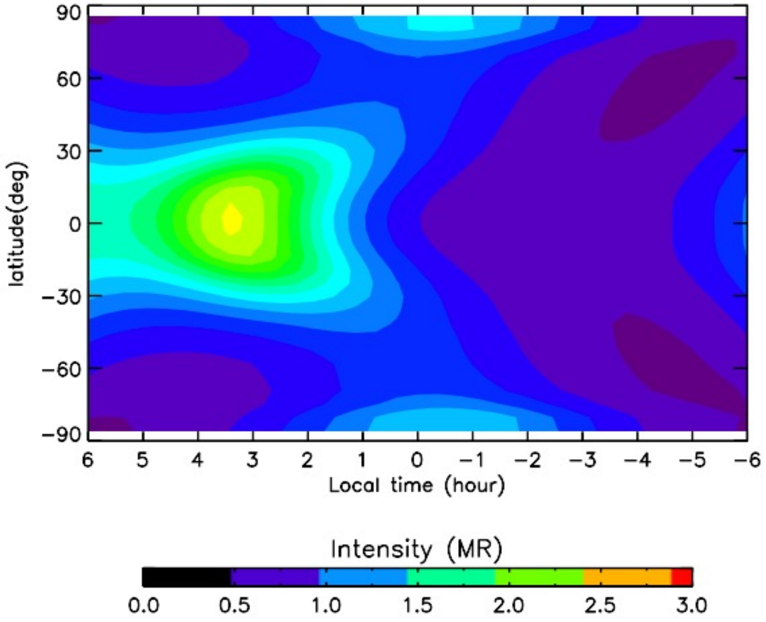

- Recent observation by VEX suggested no shift (Piccioni et al., 2009)
  → gravity wave saturation should occur in higher altitudes
- Lower intensity because of less transport of O from the dayside

Implication for wind observation

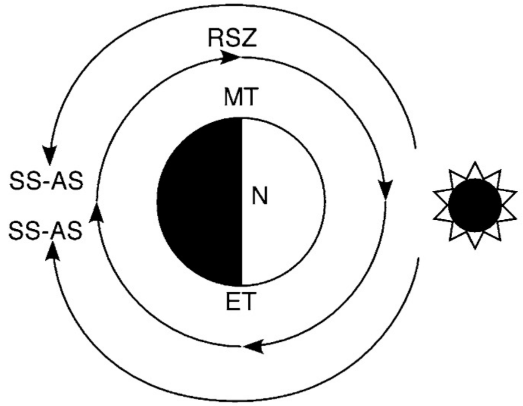

Zonal wind velocity at 110 km altitude

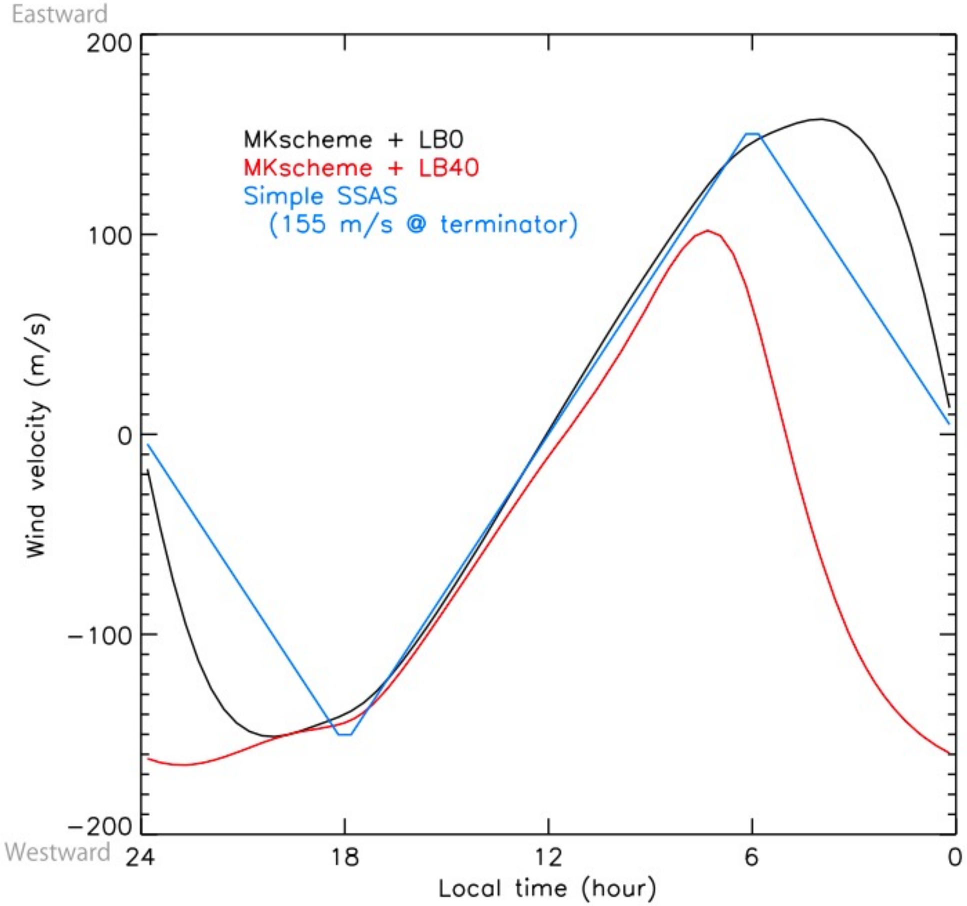

RSZ wind profile

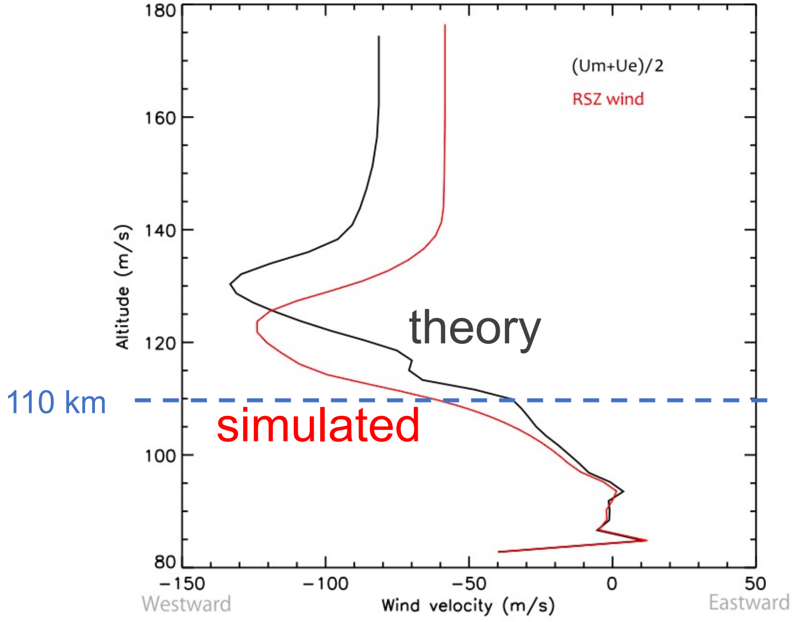

Theoritical approach

$$u_e = u_{\mathrm{RSZ}} - u_{\mathrm{SSAS}}$$
$$u_m = u_{\mathrm{RSZ}} + u_{\mathrm{SSAS}}.$$

$$u_{\mathrm{SSAS}} = (u_e - u_m)/2$$
$$u_{\mathrm{RSZ}} = (u_e + u_m)/2.$$

- Theoritical estimation can cause large error at 110 km (CO_2 10 μm emmision altitude) due to the asymmetricity of the wind field

Summary of Hoshino et al. (2012, 2013)

❑ Hoshino et al. (2012)

- Symmetric SS-AS circulation and the return flow below 90 km
- Thermal tides : small amplitude, weak vertical propagation
  Rossby waves : small amplitude, strong vertical propagation
  Kelvin waves : large amplitude, strong vertical propagation
- Kelvin wave would cause observed fluctuation of O_2 nightglow emission

❑ Hoshino et al. (2013)

- The gravity waves have an important role in controlling RSZ wind
- The gravity waves would cause larger fluctuation than that of Kelvin wave
- Theoritical estimation $\neq$ actual RSZ wind ?

Test runs and applications

Test runs of Hoshino et al. (2012, 2013)

- Hoshino et al., 2012

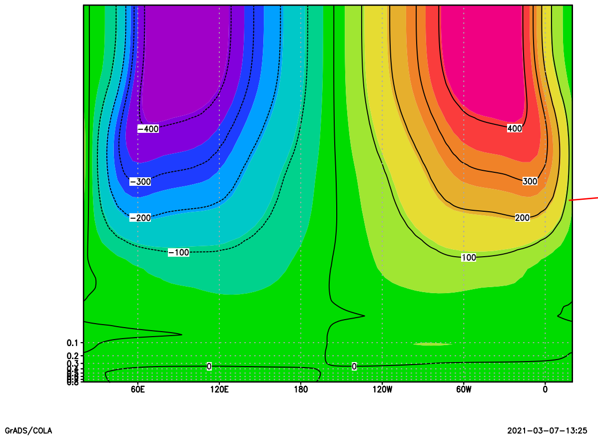

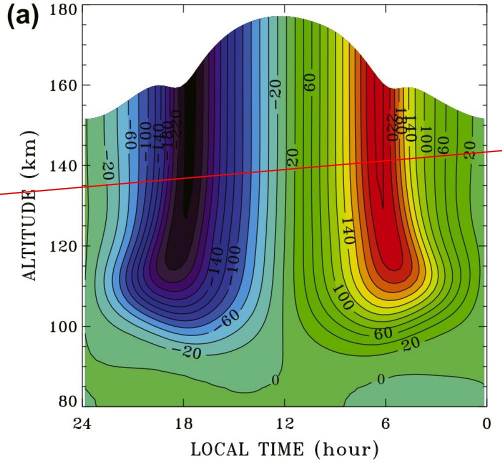

Same feature but larger amplitude
(without wave drag parameterization)

Same features and amplitudes

- Hoshino et al., 2013

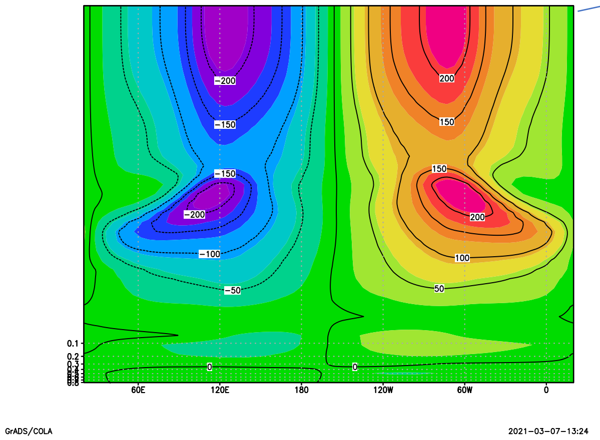

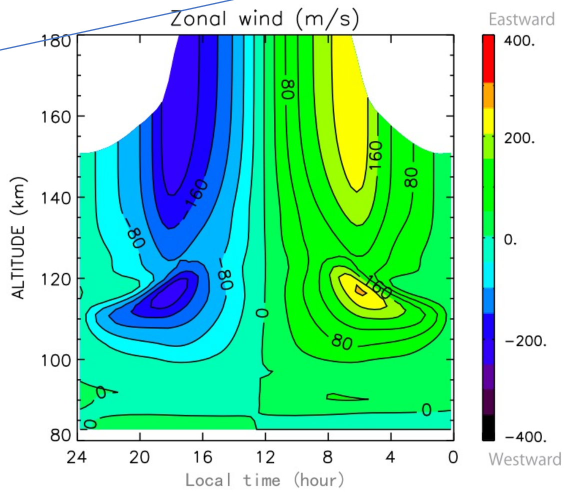

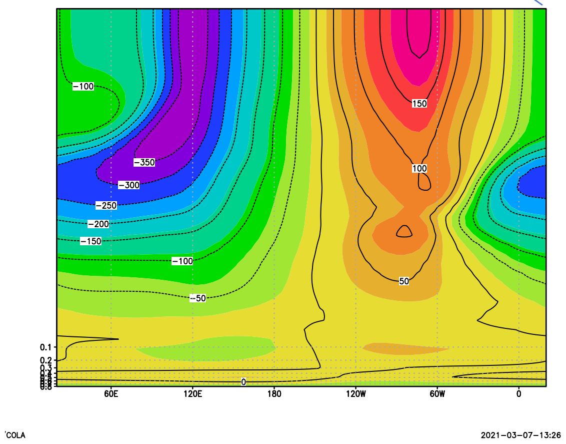

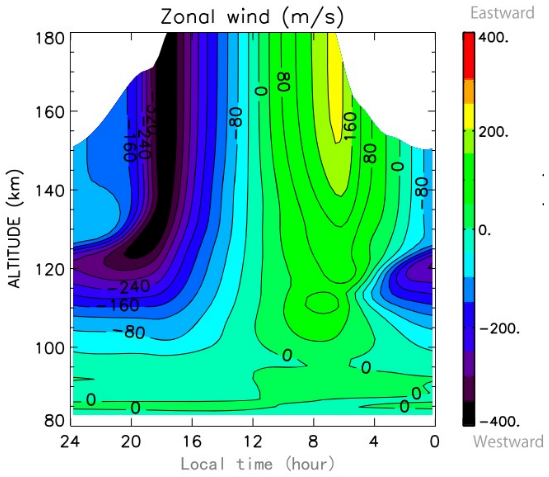

Applications

❑Coupling with a photochemical model

- Chemical reactions including SO_2, Cl, etc.
- Comparison with telescope observation

❑Coupling with a lower atmosphere VGCM

- Interaction with lower atmosphere
- Effects of radiative reactive cloud

Better understanding of general circulation and atmospheric chemistry

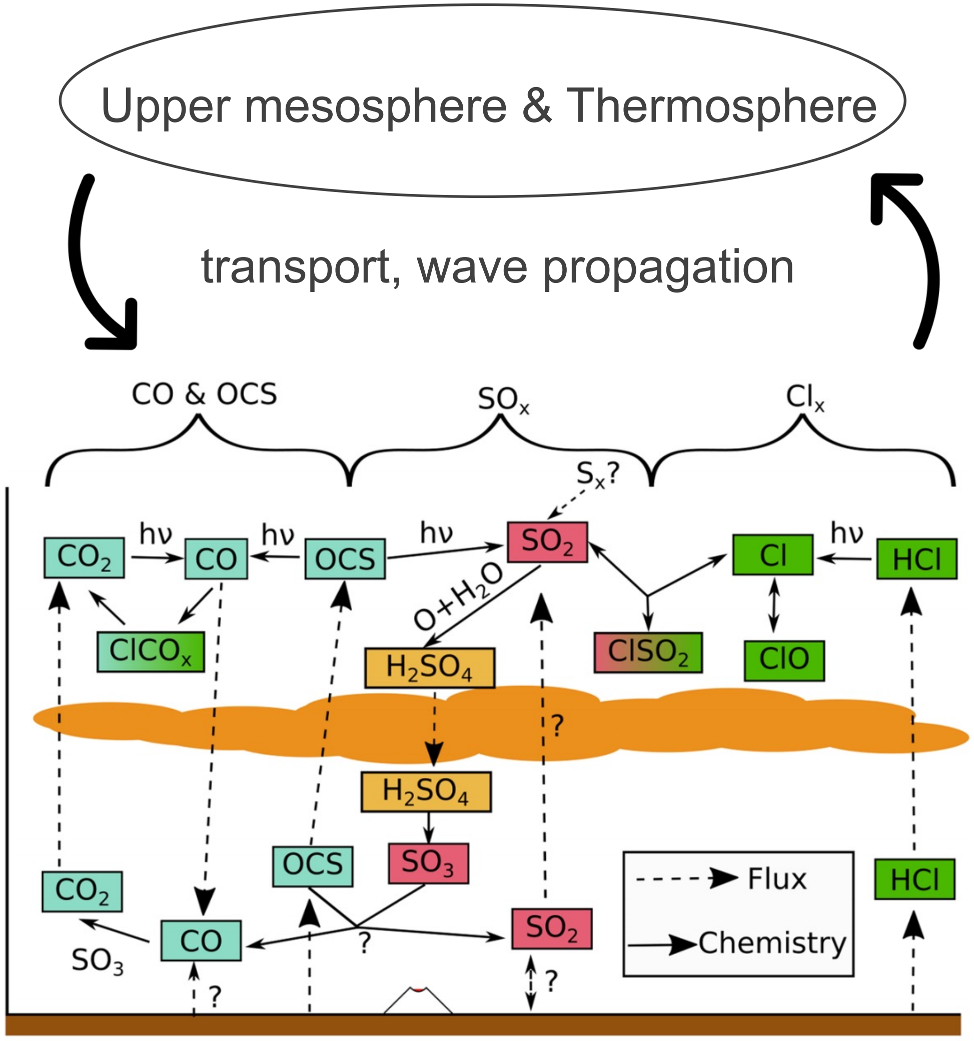

[Bierson and Zhang., 2020]